

# Information-theoretic description of a feedback-control Kuramoto model

Damian R Sowinski,<sup>1,\*</sup> Adam Frank,<sup>1,†</sup> and Gourab Ghoshal<sup>1,‡</sup>

<sup>1</sup>*Department of Physics and Astronomy, University of Rochester*

Semantic Information Theory (SIT) offers a new approach to evaluating the information architecture of complex systems. In this study we describe the steps required to *operationalize* SIT via its application to dynamical problems. Our road map has four steps: (1) separating the dynamical system into agent-environment sub-systems; (2) choosing an appropriate coarse graining and quantifying correlations; (3) identifying a measure of viability; (4) implementing a scrambling protocol and measuring the semantic content. We apply the road map to a model inspired by the neural dynamics of epileptic seizures whereby an agent (a control process) attempts to maintain an environment (a base process) in a desynchronized state. The synchronization dynamics is studied through the well-known Kuramoto model of phase synchronization. Our application of SIT to this problem reveals new features of both semantic information and the Kuramoto model. For the latter we find articulating the correlational structure for agent and environment (the oscillators), allows us to cast the model in a novel computational (information theoretic) perspective, where the agent-environment dynamics can be thought of as analyzing a communication channel. For the former we find that all the information in our system is semantic. This is in contrast to previous SIT studies of foragers in which semantic thresholds were seen above which no further semantic content was obtained.

## I. INTRODUCTION

It is generally accepted that information plays an important role in complex-adaptive, and living systems in particular [1]. From DNA transcription to signal transduction, information flows and information processing appear to be an essential aspect of living systems [2–13]. Indeed, the capacity to use information, rather than just be described in terms of it, may be the characteristic which separates life from other physical systems [14–16].

There is, however, an important caveat in making information a central component in developing a *physics of life*. Information theory, tracing its roots back to Shannon’s famous paper [17], is constructed using purely syntactic measures. Information, in this formalism, is defined in terms of the combinatorics of strings composed of letters drawn from an alphabet. Such a definition purposely ignores the question of the *semantic content* of information. While highly useful for engineering issues like the design of computational technologies, when it comes to questions associated with the emergence and dynamics of living systems, ignoring issues of meaning filters out the most important ways life uses information [18, 19]. For example, understanding the emergence of agency and autonomy revolve around the capacity of a system to parse streams of information in terms of their *valence* for the system i.e. their meaning. Indeed,

such valence, defined as *Viability* has been identified as a critical feature defining the boundary between living and non-living systems [20, 21].

While extensive discussions of, and definitions for, semantic information exist, they have mostly focused on issues in philosophy or applications within computer science [22–28]. What has been lacking for a *physics of life* is a mathematically precise and scientific applicable theory of semantic information that can inform a wide range of domains ranging from neuroscience, collective microbial behavior, social physics and Origin of Life studies [29–37].

In [38] (KW18) such a semantic theory of information (SIT) was proposed. Their formulation uses the state spaces and probability distributions for an agent  $A$  and its environment  $E$  to characterize the mutual information between the two, while the persistence of  $A$  (its ability to maintain a desired state) is measured through a real-valued viability function  $\mathcal{V}$ . The concept of meaning here is thus taken in the most basic sense of being related to an agent’s continued existence. By running *intervened* versions of the system dynamics in which some fraction of the mutual information between agent and environment is scrambled, a formal working definition of the semantic information was characterized in terms of the response of the viability function to such interventions. Importantly, the viability is determined by the inherent coupled dynamics of the system and the environment [38, 39], rather than through exogenous utility, cost, error, or loss functions (as is sometimes done when studying the value of information in statistics or in engineering applications [13, 40–42]).

The KW18 formalism appears to offer an attractive path forward for the development of a working theory

\* [Damian.Sowinski@UR.Rochester.EDU](mailto:Damian.Sowinski@UR.Rochester.EDU)

† [afrank@pas.rochester.edu](mailto:afrank@pas.rochester.edu)

‡ [gghoshal@pas.edu](mailto:gghoshal@pas.edu)

of semantic information. The difficulty, however, lies in the computational cost of applying the formalism to real world applications. Calculating the information theoretic measures, require a precise elucidation of the state spaces, and the computation of the joint probability distributions between the agent and the environment. Unfortunately such state spaces are often of such high dimensionality that the formalism is computationally intractable. Thus if SIT is to live up to its promise, work must be done to find *effective* measures for the quantities required in its formalism. This includes best practices for definitions of viability, proper mechanisms for scrambling shared information in the intervened trajectories and, finally, practical methods of dimensional reduction (i.e. coarse-graining) for calculations of information theoretic metrics.

Recently, an attempt to develop such effective versions of the KW18 formalism was presented in [43]. The authors studied a forager model, a minimal model that captures attributes of living systems, namely exploration and resource consumption [44–47]. The viability was defined as the expected lifetime of the forager and the scrambling was done by noising a sensor that the forager used to detect resources. They applied and extended the work of KW18 and demonstrated how semantic information measures provide new insights into forager dynamics. More importantly, they provided a first cut at developing effective measures for application of the SIT formalism to real problems.

An important result from [43] was the identification of a plateau in the viability curve as a function of scrambling correlations between agent and environment. This plateau occurs at a *viability threshold* that is well below channel capacity. In other words a subset of correlations between agent and environment has no effect on the forager’s lifetime (the information was not semantic). Once the threshold is breached the ability for the forager to survive decreases monotonically with increased scrambling (noise in the sensor). Thus applying the ideas of SIT results in an identification of features in the viability curve that are both novel and independent of the particular foraging strategy used. Whether such semantic saturation is a generic feature of living systems is far from settled, but the results make it clear that finding ways to apply the fundamental principle of SIT results in novel ways to analyze systems from an informational perspective.

In this paper we report on the next step in efforts to operationalize SIT and explore *effective* versions of the theory. To carry out that task we explore the biophysically motivated problem of a control process (CP) acting on a base process (BP) to maintain over-

all system viability. We analyze a model of a network of coupled oscillators which tend towards synchronization (the base process) and an intervening agent (the control process) which uses the information on the network to limit synchronization. The synchronization dynamics is studied through the well-known Kuramoto model of phase synchronization [48]. This setting is loosely inspired by the neurodynamics of epileptic attacks [49–52] where brain pathologies occur due to large scale synchronization of neurons [53]. Additionally, in versions of the Kuramoto model with non-local coupling [54] or symmetry-breaking [55] there exist chimera states, where identically coupled oscillators coexist in synchronized and desynchronized states. Such states have been observed in both brain networks and the resuscitation of cardiac cells [56]. Thus desynchronization is important in many biological contexts. Consequently, the intervening agent here acts as preventing the system from reaching (a potentially) pathological synchronized state. Our goal in this paper, as in [43], is to both explore the application of the KW18 formalism and use SIT to shed new light on a previously well-studied problem, phase-(de)synchronization.

In what is to follow, in Sec. II we explicitly unpack the general steps required for the use of the SIT formalism. In Sec. III A we introduce the feedback-control model on the coupled oscillators. We demonstrate that introducing the agent leads to a stochastic version of the original Kuramoto model, with oscillators coupled to a heat-bath mediated by their degree  $k_i$  and a deformed distribution of frequencies  $g(\omega)$ . Following this in Sec. III B we recast the model in information theoretic terms in which we show that the base process is a stochastic computation, and the control process is akin to analysing a communication channel between the agent and its environment. The viability function is defined in Sec. III C and in Sec. III D we analyze the semantic content of the correlations between agent/environment demonstrating the absence of a semantic threshold, indicating that every bit of information in the communication channel is crucial to the viability of the system. Finally in Sec. IV we end with a discussion of the implications of our findings. Three Appendixes clarify technical aspects of our model and the approximations used.

## II. PRELIMINARIES

Here we provide a set of general set of steps for applying semantic information theory to any framework.

- **Dynamical System Decomposition.** Construct a *dynamical system*  $(S, \mathcal{D})$ , where  $S$  is

the system state space and  $D : S \times T \rightarrow S$  is the dynamics on the state space for all times  $t \in T$ . The dynamics can be deterministic, stochastic, or a combination of the two; if they are continuous then  $T \simeq \mathbb{R}$  or some subinterval of the reals, and if they are discrete then  $T \simeq \mathbb{Z}$ , or some finite subsequence of the integers. The system must be factorable into an *agent* and *environment*,  $S = A \times E$ , meaning that any state of the system can be written  $s = (a, e)$  where  $a = (a_1, a_2, \dots) \in A$  and  $e = (e_1, e_2, \dots) \in E$  are, respectively, the agent and environment dynamical degrees of freedom (DoF). We write  $s(t) = (e(t), a(t))$  to represent the system evolution through state space, and refer to the specific form of  $\mathcal{D}$  responsible for  $a(t)$  as the agent’s *behavior*.  $S$  needs to accommodate a (not necessarily unique) ground state for the agent which acts as an attractor for the system dynamics and represents a *dead* agent and an evolving *agent-free* environment.

- **Coarse Grain and Quantify Correlations.** Correlations between agent and environment DoF are manifest in the information architecture of the system, as quantified by a corpus of measures including mutual information,  $I(A : E)$  [57], cross entropy  $H(A : E)$  [58], and transfer entropy  $\mathcal{T}_{E \rightarrow A}$  [59]. In practice these quantities may not be calculable or efficiently computable in full, so a bit of finesse is required at this step. A combination of prior knowledge and intuition must be used to coarse grain the system into DoF that lend themselves to the desired analytical or computational techniques, while capturing the minimal dynamics of  $S$  required to describe an agent attempting to survive in and coevolve with its environment. In particular, the agent-free attractor must be preserved by the coarse graining. For example, it would be intractable to describe a bacterium’s environment by listing the position and momentum of every atom surrounding it; a simpler description using a coarse-grained glucose density field might suffice. Describing the full biochemistry of the bacterium using every molecular DoF is intractable, but a coarse grained smaller set of DoF such as *center of mass position*, *orientation*, *stored ATP density*, and *locomotive modality* may not be. Note how this coarse-graining preserves the ground state: in the limit when the bacterium’s stored ATP supply vanishes it is effectively dead.
- **Identify Viability Measure  $\mathcal{V}$ .** Since the ground state remains an attractor for the system dynamics under coarse graining, the *dis-*

*tance* to it endogenously defines the *viability* of an agent. *Distance* here can mean several things: If the attractor is stable, then an agent trajectory will eventually end up on it, i.e. the agent will die. In this case the expected lifetime of the agent is a proper measure of distance, and hence viability. The example of the bacterium falls in this case; the expected first crossing time to reach zero ATP supply is a viability measure. If the attractor is unstable, then the coarse graining from the prior step must be able to identify an order parameter representing the *efficacy* of the agent at maintaining an out-of-(agent-free)equilibrium environment. The efficacy vanishes in an agent-free environment, and takes some non-zero value once the agent is introduced. The expected efficacy is then a proper measure of distance, and hence viability. The viability of the agent measured in either case is referred to as the *actual viability*.

- **Scrambling Protocol and measuring semantic Content.** The goal of SIT is to identify how the correlations and viability defined in the last two steps relate to one another. Specifically, to find which correlations matter to the agent. This is done by implementing a scrambling protocol on the correlations, and examining the resultant change in viability due to the impact the scrambled correlations have on the dynamics of the system. This was expounded on in KW18 using *interventions* to generate counterfactual histories, and requires a search over all possible partitions of the system degrees of freedom. Though rigorously defined, the procedure becomes unmanageable for systems with more than several hundred states. Rather than going through all partitions, the coarse graining, if done correctly, identifies which coarse-grained DoF should be investigated and scrambled. In the example mentioned earlier, the bacterium’s orientation and whether it is tumbling or rolling are correlated to gradients and magnitudes of the glucose density. A scrambling protocol could be introduced at the level of the dynamics by intervening on the bacterium’s ability to sense either a magnitude or a gradient, or on the conditions that determine when the bacterium should switch it’s locomotive modality. The protocol should be tuneable, in the sense that the actual viability is a limiting case. To contrast with the actual viability, the scrambled viability is measured as the protocol is tuned higher. The point at which the scrambled viability diverges from the actual viability is the *semantic threshold* [43].

### III. KURAMOTO MODEL WITH FEEDBACK-CONTROL

Kuramoto's famous coupled oscillator model has been well-studied since its introduction nearly half a century ago [48]. From the synchronization of fireflies, cardiac pacemakers, laser, power transmission relay networks among others, it has proven a rich starting point for modelling systems in which synchronization is prominent [60–63]. Above a critical coupling strength, an extensive fraction of oscillators achieve an equilibrium synchronized state, while the desynchronized states are non-equilibrium transients in the dynamics. As mentioned in the introduction, the phenomenon of *desynchronization* has biological relevance in terms of pathological states in the human brain and in cardiac arrhythmia. Inspired by this, we develop a feedback-control model of an agent acting on a population of coupled oscillators that attempt to *prevent synchronization*. We then apply the SIT framework to this idealized model and develop a new information theoretic perspective on coupled oscillators. In our formulation, the control process (an agent) seeks to drive the base process (the Kuramoto model) to a desired far-from-equilibrium set of states. Remaining far-from-equilibrium provides a definition of viability i.e. it motivates the teleological dynamics of the agent (the control process) seeking to keep the system from complete synchronization. Viewing the system through the lens of semantic information the agent can be interpreted as a repair process acting on a malfunctioning background.

#### A. Dynamical System Decomposition

##### 1. Environment Description

The environment is a population of  $N$  oscillators  $(\theta_1 \dots \theta_N)$ ,  $\forall i, \theta_i \in (-\pi, \pi]$  placed on the nodes of an undirected graph  $G$  with connections parameterized by the adjacency matrix  $\mathbf{A}$  whose elements are  $A_{ij} = 1$  if nodes  $i$  and  $j$  are connected, and 0 otherwise. In what is to follow, we consider Poisson and scale-free degree distributions generated via the configuration model [64]. The oscillators are coupled to one another with a coupling  $\sigma$ , which we take to be a function of time. Each oscillator has a natural frequency,  $\omega_i$ , drawn from a distribution  $g(\omega)$ . Without loss of generality we set  $\langle \omega \rangle = 0$ . The variance, or more precisely the root mean square frequency  $\omega_{\text{rms}} = \langle \omega^2 \rangle^{1/2}$ , is used to rescale time,  $\tilde{t} = \omega_{\text{rms}} t$ . Dropping the tildes, the dynamics of the dimensionalized environment are the Kuramoto equations of

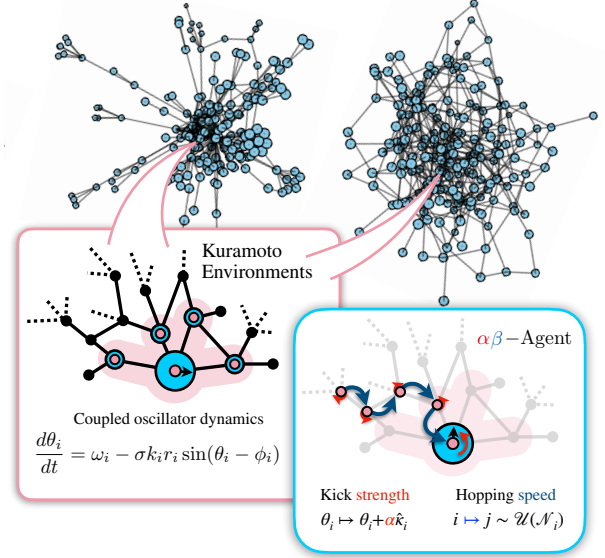


FIG. 1. Oscillators  $\{\theta_i\}$  are placed on the nodes of both power law (upper left) and Poisson graphs (upper right). Kuramoto dynamics are imposed resulting in Kuramoto environments. At each node (lower left) there is a local order parameter and local mean field,  $\{r_i, \phi_i\}$ . Together, these dynamical quantities define the local mean field coupling for each oscillator of natural frequency  $\omega_i$ . Control agents are placed in the Kuramoto environments, moving uniformly at random along edges, and perturbing the nodes based off of local mean field estimates  $\phi_i$ . Here  $\alpha$  describes the strength of the perturbation that the agent applies, and  $\beta$  the time-scale or speed of the perturbation.

motion, thus,

$$\frac{d\theta_i}{dt} = \omega_i + \sigma \sum_{j=1}^N A_{ij} \sin(\theta_j - \theta_i), \quad (1)$$

with  $g(\omega)$  having vanishing mean and unit variance.

##### 2. Agent Description

The agent is a localized, mobile perturbation whose purpose is to maintain a global desynchronized state. The agent's degrees of freedom are  $a = (i, \kappa_i)$ , where  $i$  is the index of the node it is at, and  $\kappa_i \in \{\pm 1\}$  is the direction of a perturbation of *strength*  $\alpha$  it applies to the oscillator at  $i$ . After perturbing, the agent *jumps* to an adjacent node uniformly at random; the entire jump-perturbation action takes a time much shorter than the environmental timescale,  $\tau \ll 1$ , but not so fast that it can perturb more than a small fraction of the network on that same timescale,  $\tau \gg 1/N$ .



This gives a natural way to parametrize the *speed* of the agent as  $\beta = 1/N\tau \ll 1$ . As we will show, the single parameter  $\alpha\beta$ , fully describes the behavior of an agent. A schematic of the process is shown in Fig. 1.

### 3. Dynamics

We begin with the dynamics of the environment. A global order parameter defined in terms of the synchronization  $r$ , and mean field  $\phi$  is constructed thus,

$$re^{i\phi} = \frac{1}{N} \sum_{j=1}^N e^{i\theta_j}. \quad (2)$$

Analogously, local order parameters and mean fields are introduced via

$$r_i e^{i\phi_i} = \frac{1}{k_i} \sum_{j=1}^N A_{ij} e^{i\theta_j}, \quad (3)$$

where  $k_i = \sum_j A_{ij}$  is the degree of node  $i$ . In the fully-connected Kuramoto model,  $\sigma = K/N$ , and Eq.(1) describes a set of oscillators that interact solely through their mutual coupling to the mean field,

$$\frac{d\theta_i}{dt} = \omega_i - Kr \sin(\theta_i - \phi). \quad (4)$$

For arbitrary network topologies one can show that Eq.(1) can be written in an analogous way using the local order parameters [65],

$$\frac{d\theta_i}{dt} = \omega_i - \sigma k_i r_i \sin(\theta_i - \phi_i). \quad (5)$$

In the thermodynamic limit,  $N \rightarrow \infty$ , in the fully-connected model, above a critical coupling ( $K_c = 2/\pi g(0)$ ) oscillators begin to synchronize,  $r > 0$ . Analysis of mean field formulations for more complex topologies suggest that  $\sigma_c = K_c \langle k \rangle / \langle k^2 \rangle$ , where  $\langle k^n \rangle$  is the  $n^{\text{th}}$  moment of the degree distribution of  $G$ . Numerical results suggest a more complicated relationship with topology, while confirming that  $\sigma_c \propto K_c$ . In our model the coupling is driven exogenously, that is perturbations to the system from outside of itself can drive  $\sigma$  to values above and below  $\sigma_c$  (for instance exposure to stroboscopic lights triggering an epileptic fit, or magnetic fields altering cardiac rhythm). Of interest to us will be when the system transitions through the critical coupling from below, shifting the system equilibrium to synchronized states. As the environment slides towards its

new equilibrium, the agent as a control process, seeks to maintain a desynchronized state. Thus it must tune its actions towards that goal, while only using local information, that is knowledge only of the location  $i$  (the node) and its immediate neighborhood.

The agent at node  $i$  has access to the phase of the oscillator  $\theta_i$ . It estimates the mean field due to the neighboring oscillators,  $\hat{\phi}_i$ , and compares it to  $\theta_i$ . If  $\theta_i > \hat{\phi}_i$ , the agent perturbs the oscillator by changing its phase positively, whereas if  $\theta_i \leq \hat{\phi}_i$  it perturbs it in the opposite direction. More precisely we have  $\theta_i \mapsto \theta_i + \alpha \kappa_i$ , where  $\alpha$  is the strength of the agent's perturbation and

$$\kappa_i = \begin{cases} +1 & \text{if } \theta_i > \hat{\phi}_i \\ -1 & \text{otherwise} \end{cases} \quad (6)$$

### 4. Agent-effect on synchronization dynamics

We simulate an ensemble of agents with  $\alpha = 0.5$  and  $\beta = 0.01$  on two types of graphs, with the same average degree  $\langle k \rangle$  but increasing degree-variance  $\sigma_k^2 = \langle k^2 \rangle - \langle k \rangle^2$ . (See Appendix A for details of the simulation.) In Figure 2 we plot the global order parameter  $\mathbb{E}[r]$ , as a function of the coupling strength  $\sigma$ . The dashed curves represent the Kuramoto environment without the agent, whereas the solid curves represent agent incorporation. In all three cases we see the effect of the agent is to delay the onset of synchronization, with the most dramatic suppression seen in the scale-free graph. Simulations varying  $\alpha, \beta$  exhibit strikingly similar behavior between an  $(\alpha, \beta)$  agent and a  $(\alpha', \beta')$  agent if  $\alpha\beta = \alpha'\beta'$ .

To get an analytical handle on why this degeneracy occurs, we incorporate the discrete agent dynamics, Eq. (6), into the continuous dynamics of the environment, Eq.(1). The specifics are in Appendix B, but the end result is the stochastic differential equation,

$$\begin{aligned} \frac{d\theta_i}{dt} = & \omega_i - \sigma k_i r_i \sin(\theta_i - \phi_i) \\ & + \alpha\beta \frac{k_i}{\langle k \rangle} \kappa_i + \sqrt{\alpha\beta \frac{k_i}{\langle k \rangle}} \frac{dW_i}{dt}, \end{aligned} \quad (7)$$

where  $W_i$  is a Wiener process. Incorporation of an agent leads to the addition of two dynamical terms in Eq. (1) parametrized by the perturbation strength and timescale  $\alpha$  and  $\beta$ , respectively. Both parameters enter in solely through their product, providing an explanation for the observed degeneracy.

The two additional terms in Eq. (7) have interesting physical interpretations. The second one plays

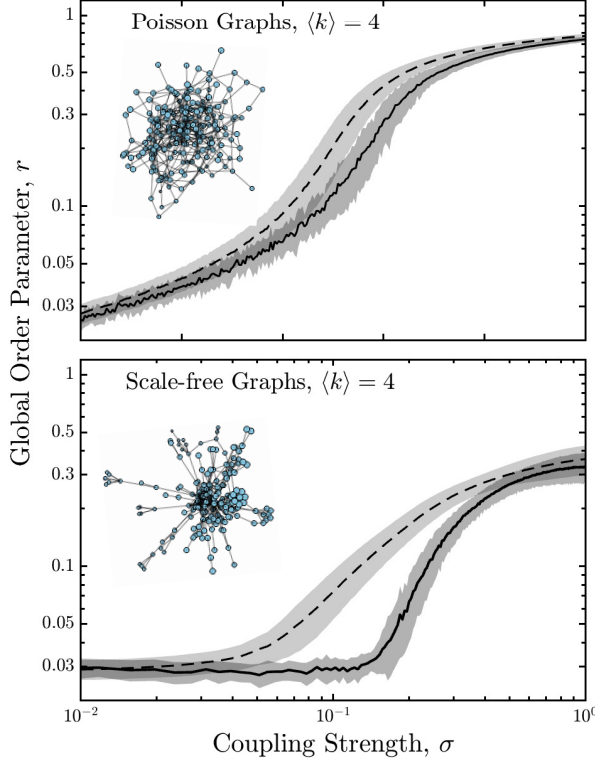


FIG. 2. The expected global order parameter for Poisson (top), and scale-free (bottom) graphs ( $N = 10^3$ ) as a function of the coupling strength  $\sigma$ . All networks have an average degree  $\langle k \rangle = 4$ . The dashed curves represent a pure Kuramoto environment, while the solid curves represent the incorporation of the intervening agent. In both cases the shaded regions represents  $1\text{-}\sigma$  fluctuations from an ensemble computation. Note that the vertical axis scales logarithmically on all the plots, while the horizontal axis is linear for the top plot and logarithmic on the bottom one.

the role of a heat bath as in other variants of the Stochastic Kuramoto model [66, 67]. The key difference here is that the strength of the fluctuations at location  $i$  is modulated by the degree of the node  $k_i$ . Instead of a single heat bath, there are several at temperatures quantized in units of  $1/\langle k \rangle$ . Nodes with higher degree are coupled to hotter baths, while those with lesser degree to colder ones.

What about the first additional term? For an oscillator to synchronize, Eq. (5) implies it's natural frequency satisfies  $|\omega_i| \leq \sigma k_i r_i$ . When  $\omega_i$  is positive, the oscillator will do so ahead of the mean phase, while for negative  $\omega_i$  it will do so behind the mean phase; put simply  $\omega_i$  has the same sign as  $\kappa_i$ . Therefore the term effectively shifts the natural frequencies

of synced oscillators to larger values,

$$\omega_i \mapsto \begin{cases} \omega_i + \alpha \beta \frac{k_i}{\langle k \rangle} & \omega_i > 0, \\ \omega_i - \alpha \beta \frac{k_i}{\langle k \rangle} & \omega_i < 0. \end{cases} \quad (8)$$

This shift changes the synchronization criterion to  $|\omega_i| < \sigma k_i r_i - \alpha \beta k_i / \langle k \rangle$ . Oscillators with positive natural frequencies between  $\sigma k_i r_i - \alpha \beta k_i / \langle k \rangle < \omega_i < \sigma k_i r_i$  or negative natural frequencies between  $-\sigma k_i r_i < \omega_i < -\sigma k_i r_i + \alpha \beta k_i / \langle k \rangle$  that were synchronized in the absence of an agent will desynchronize in the presence of one. Consequently the local order parameters,  $r_i$ , decreases, causing a cascade of oscillators inside the old synchronization range to follow suit until a new equilibrium is reached.

The combined effect of the two agent terms in Eq. (7) can best be understood qualitatively via their effect on the frequency distribution,  $g(\omega)$ . The heat bath alone acts as a Gaussian convolution kernel, which is then shifted as per Eq. (8). For any reasonable initial distribution  $g$  convolved with the kernel  $h$ , results in a deformed distribution,  $g^A = h * g$  of higher variance ( $*$  is the convolution operator). This deformation stretches the distribution and, to conserve probability, compresses its height such that  $g^A(0) < g(0)$ . Given that  $\sigma_c^A / \sigma_c = K_c^A / K_c = g(0) / g^A(0) > 1$ , the critical coupling in the presence of the agent increases which, in turn, delays the onset of synchronization.

## B. Coarse-graining and quantifying correlations.

The full state space of our system is  $S = (-\pi, \pi]^N \times \{1, 2, \dots, N\} \times \{\pm 1\}$ . The last of these describe the agent's action  $\kappa_i$ , based on their observation of the local mean field  $\hat{\phi}_i$ . Combining this with  $\theta_i$ , the agent determines whether oscillator  $i$  is running ahead or behind the mean field of its neighbors. For the agent, the state space of the environment is coarse grained to a string of bits  $\mathbf{b}$ . The action of the agent depends on the outcome of its measurement, and the maximal mutual information between the environment and the agent's action degree of freedom is one bit per jump. The  $i^{\text{th}}$  bit  $b_i$  is 1 if the oscillator at the  $i^{\text{th}}$  node is running ahead of its mean field, or 0 otherwise.

As the oscillators evolve, the bits corresponding to synchronized oscillators remain fixed, whereas bits corresponding to unsynchronized oscillators flip pseudo-randomly. In this light, the Kuramoto model with feedback control can be reduced to two coupled stochastic computations. The timescale between flips of the computing bits from Eq.(5), under a steady

state assumption on both  $r_i$  and  $\phi_i$ , is half an oscillators period

$$\begin{aligned}\tau &= \frac{1}{2} \int_0^\tau dt = \frac{1}{2} \int_{-\pi}^\pi d\theta \frac{1}{\dot{\theta}} \\ &= \frac{\pi}{\sqrt{\omega_i^2 - \sigma^2 k_i^2 r_i^2}}.\end{aligned}\quad (9)$$

As  $\sigma$  approaches the critical coupling  $\sigma_c$ , there is a slowing down of the computation due to the divergence of the time-scale  $\tau \sim (\sigma_c - \sigma)^{-1/2}$ . As the equation indicates, nodes with high connectivity (i.e. hubs) have the longest bit-flip timescales, whereas lower-degree nodes compute on a faster time-scale.

Given this view of the environment as a base computational process,  $\mathbf{b} \mapsto \mathbf{b}'$ , the agent is a control process, and the estimation of the mean field at each node maps to the problem of analyzing a communication channel. The channel's operational rate is  $\beta N$ , achieved if the environment has a uniform, i.e. maximum entropy input distribution. Synchronization changes the input distribution by lowering its entropy—synchronized bits decrease the corpus of words being sent. If the agent decodes with high fidelity, then its actions' feedback on the environment is to prevent changes in the input distribution. Thus the control process serves to prevent the reduction of the channel's transmission rate.

Putting it together, the background process (environment) transmits at a rate of close to  $\beta N$  (bits/s) to the control process (agent). Synchronization reduces the transmission rate, to which the control process responds in a manner that counteracts this change. To address what portion of this information is semantic, we next identify precisely what we mean by viability in this context.

### C. Viability Measure $\mathcal{V}$

As indicated by Fig. 2 the agent-free equilibrium has an expected synchronization greater than the agent-present equilibrium. The effectiveness of the agent at keeping the environment asynchronous, defines its ability to keep the system viable. This provides us with a natural choice within the system dynamics for defining viability in terms of efficacy.

The *efficacy* is the relative difference between the expected value of the synchronicity of the environment including the agent ( $\mathbb{E}[r|\alpha, \beta]$ ) and without it ( $\mathbb{E}[r]$ ) thus,

$$\mathcal{E} = 1 - \frac{\mathbb{E}[r|\alpha, \beta]}{\mathbb{E}[r]}.\quad (10)$$

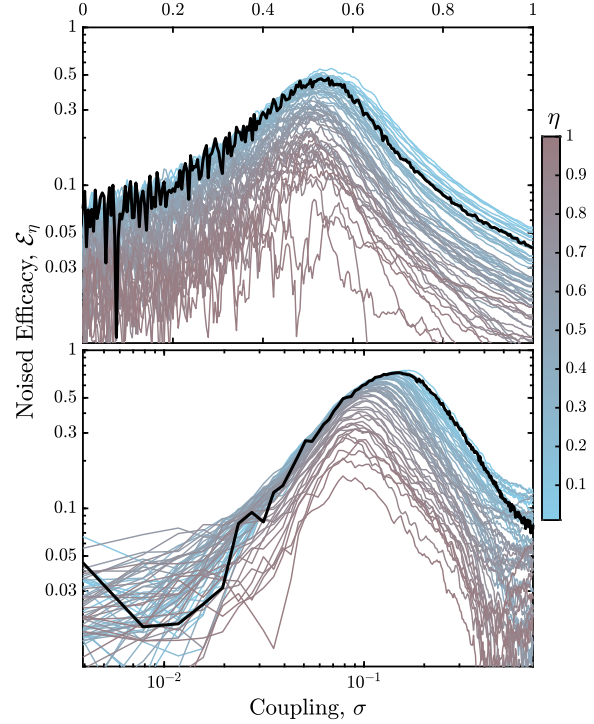


FIG. 3. The efficacy, Eq. (10) (solid black lines), for agents on Poisson graphs (top panel) and scale-free graphs (bottom panel) with  $\alpha = 0.5$  and  $\beta = 0.01$ . The noised efficacies, Eq. (17), are shown as colored curves with blue corresponding to low noise and pink to high noise. The curves are averaged over an ensemble of 128 graphs for each value of coupling and noise.

Given that  $r$  is a function of  $\sigma$ , this necessarily implies that the efficacy is also a function of the coupling. The more the agent's actions decrease the expected synchronization, the closer the efficacy is to 1 whereas if the agent is completely ineffectual, the efficacy is 0. The *viability*, then, is the expected efficacy given the distribution of possible coupling strengths,  $\rho(\sigma)$ ,

$$\begin{aligned}\mathcal{V} &= \mathbb{E}_\sigma[\mathcal{E}] \\ &= \int_0^\infty d\sigma \mathcal{E}(\sigma) \rho(\sigma).\end{aligned}\quad (11)$$

In Fig. (3), we plot the efficacy (Eq. (10) as solid black lines in function of  $\sigma$  for both types of networks. In all cases we see a non-monotonic behavior, with a peak in  $\mathcal{E}$  at intermediate values of  $\sigma$ . Qualitatively speaking, for low values of the coupling ( $\sigma \ll \sigma_c$ ) the effect of the agent is minimal given that the system is in an asynchronous state and therefore there is no need to intervene. On the other hand in the strong coupling regime  $\sigma \gg \sigma_c$ , the agent also has low efficacy—given that  $\beta \ll 1$ , a large fraction of nodes synchronize at a timescale faster than its

ability to influence these nodes. Thus there is a peak in viability at intermediate values of  $\sigma$  where the agent can exert its strongest influence in preventing the synchronization of a non-negligible fraction of oscillators.

It is instructive to check whether the peak in efficacy occurs at (or near) the critical coupling  $\sigma_c$ . While an analytical treatment for complex topologies is difficult, progress can be made by resorting to the fully-connected version of the Kuramoto model, for which  $\sigma = K$ . As noted in Sec. III A the  $\alpha\beta$ -agent stretches the frequency distribution  $g(\omega)$ , increasing its variance from unity to  $1 + \alpha\beta$ . The derivatives of the frequency distribution at  $\omega = 0$ , namely  $g^{(2n)}(0)$  (see appendix C for details), define the critical coupling and the behavior of the order parameter near it,

$$r(K) = 2\sqrt{2\frac{g(0)}{|g''(0)|}} \frac{(K - K_c)^{1/2}}{K^{3/2}}. \quad (12)$$

We next calculate the effect of the change in variance of  $g(\omega)$  on these derivatives.

Denoting the stretched distribution  $\tilde{g}(\omega)$ , a Gaussian with variance  $1 + \alpha\beta$ ; we relate it to the original distribution in the limit  $\alpha\beta \ll 1$ :

$$\begin{aligned} \tilde{g}(\omega) &= \frac{e^{-\frac{1}{2(1+\alpha\beta)}\omega^2}}{\sqrt{2\pi(1+\alpha\beta)}} \\ &\approx \left(1 + \frac{\omega^2 - 1}{2}\alpha\beta\right) g(\omega). \end{aligned} \quad (13)$$

The critical coupling of the deformed distribution,  $\tilde{K}_c$ , is consequently shifted according to,

$$\tilde{K}_c = \frac{2}{\pi\tilde{g}(0)} \approx K_c \left(1 + \frac{\alpha\beta}{2}\right). \quad (14)$$

For environments with coupling below  $K_c$ , the agent is not effective because the environment dynamics are already driven towards asynchronous states. However, for  $K_c < K < \tilde{K}_c$ , the efficacy jumps to 1 since  $\mathbb{E}_{\alpha\beta}[r]$  vanishes while  $\mathbb{E}[r]$  does not. At larger couplings the agent+environment synchronization begins to drop. To first order in  $\alpha\beta$ , the efficacy can be approximated as

$$\mathcal{E} \approx \begin{cases} 0 & K < K_c \\ 1 & K_c \leq K < \tilde{K}_c \\ \frac{\alpha\beta}{4} \frac{1}{\frac{K}{K_c} - 1} & K \geq \tilde{K}_c. \end{cases} \quad (15)$$

Thus, as also seen in the simulations of more complex topologies in Fig. 3, the efficacy is peaked above the critical coupling of the agent-free environment  $\sigma_c$ , and decreases beyond the critical coupling of

the agent-inclusive environment  $\tilde{\sigma}_c$ . Based on these results we are now able to both define viability and characterize how it responds to agent dynamics. To derive semantic information content in the system we now explore the architecture of correlations in the agent/environment coupling.

#### D. Scrambling protocol and semantic content.

With the computational description in mind, a natural way of scrambling presents itself. A noisy channel reduces the information transmission rate, and therefore, the control process will not be able to modulate its behavior in a way that reduces synchronization in the background process, thus affecting its viability. Consequently, scrambling the correlations between agent and environment can be implemented by introducing noise in the agent's information about the phase of the neighborhood of node  $i$  that it visits.

Let this noise be parameterized by  $\eta \in [0, 1]$ , where  $\eta = 0$  corresponds to the agent with  $\hat{\phi}_i = \phi_i$ , and  $\eta = 1$  an agent for whom  $\hat{\phi}_i$  is drawn uniformly randomly between  $-\pi$  and  $\pi$ . For values  $0 < \eta < 1$ , the estimator is a random variable  $\hat{\phi}_i \sim \mathcal{U}(\phi_i - \eta\pi, \phi_i + \eta\pi)$ . Then for node  $i$ , defining  $\eta_c = \min(|\theta_i - \phi_i|/\pi, 1 - |\theta_i - \phi_i|/\pi)$ , the probability that the agent's kick is in the wrong direction is

$$p(\hat{\kappa}_i \neq \kappa_i | \phi_i, \theta_i) = \begin{cases} 0 & \text{if } \eta \leq \eta_c \\ \frac{1}{2}(1 - \frac{\eta_c}{\eta}) & \text{if } \eta_c < \eta < 1 - \eta_c \\ 1 - \frac{1}{2\eta} & \text{otherwise} \end{cases}. \quad (16)$$

For unsynced oscillators  $|\theta_i - \phi_i|$  takes on all values between  $\pm\pi$ , so  $\eta_c$  will take on values throughout  $[0, 0.5]$ . There will be intervals in each period of these oscillators where the agent may make mistakes. For synchronized oscillators,  $\eta_c = |\sin^{-1} \omega_i / \sigma k_i| / \pi$ . On these, neglecting the back reaction on the network, the agent will continue functioning until  $\eta = \eta_c$ , at which point, there will be errors in its ability to judge which action to take.

Averaged over all nodes visited by the agent per unit time, the contribution due to noising from both synced and unsynced oscillators further reduces the information transmission rate from environment to agent. To quantify the effect of scrambling on the viability we modify Eq. (10) by defining the noised efficacy

$$\mathcal{E}_\eta = 1 - \frac{\mathbb{E}[r|\alpha, \beta, \eta]}{\mathbb{E}[r]}, \quad (17)$$



where the expectation in the numerator of the second term is still taken over an ensemble of  $\alpha\beta$ -agents but ones whose mean field estimators have a degree of noise,  $\eta$ . Note that  $\mathbb{E}[r|\alpha, \beta, \eta = 0] = \mathbb{E}[r|\alpha, \beta]$ , so  $\mathcal{E}_0 = \mathcal{E}$ .

We plot the results of introducing noise in Fig. (3) which shows the change in efficacy (colored solid lines) in the range  $0 \leq \eta \leq 1$ . For both networks, the peak efficacy is reduced by an order of magnitude for maximal noising; while the overall shape of the curve is preserved with increased noise the curve is increasingly flattened. Note that even at maximal noising, where the agent has no correlations with the environment, the efficacy is still finite. This is easy to understand in terms of the agent acting as a heat bath—even though it is no longer making an informed choice in the way it kicks its local oscillator, the net effect is still to deform the frequency distribution enough to increase the critical coupling to  $\tilde{\sigma}_c > \sigma_c$ , and thus delay the onset of synchronization.

As before, the noised efficacy is a function of the coupling strength  $\sigma$ , so the scrambled viability is the expected noised efficacy over the distribution of possible couplings,

$$\mathcal{V}_\eta = \int_0^\infty d\sigma \mathcal{E}_\eta(\sigma) \rho(\sigma). \quad (18)$$

Without loss of generality, we assume a uniform  $p(\sigma)$  with support  $\sigma \in [0, 1]$  when computing the viabilities. The efficacy as a function of both scrambling (measured as amount of unscrambled bits) and the coupling is shown in the top panels of Fig. 4, with the light blue regions corresponding to those of high efficacy. The width of the regions is highest for low scrambling, and it tapers as the amount of scrambled information increases. We note that in both cases, the region of peak efficacy is relatively unchanged with increasing noise  $\eta$ . The high-efficacy region occurs for lower coupling strength in the scale-free case, but this is to be expected since  $\sigma_c^{\text{scale-free}} < \sigma_c^{\text{Poisson}}$  as  $\langle k^2 \rangle^{\text{scale-free}} > \langle k^2 \rangle^{\text{Poisson}}$ .

Integrating over all coupling strengths, the viability, is shown in the bottom panels of Fig. 4. In both cases, we see a linear decrease in  $\mathcal{V}$  with increasing  $\eta$ . The best linear fits to the curves (plotted as pink dashed lines), imply a constant viability per bit (VpB) in the agent/environment communication channel. For Poisson graphs VpB is found to be  $0.171 \pm 0.002$ , while for scale-free graphs  $0.209 \pm 0.003$ . Note that in the absence of noise, the presence of an agent that can accurately estimate the local mean field, has a net effect of lowering the global synchronization  $\approx 20\%$  across the given range of coupling parameters. This appears to be independent of the topology, although the decrease in viability with noise is more

pronounced in the scale-free case. This is likely due to the fact that the agent spends most of its time located in the hubs (given that the probability to visit a node  $i$  in a random walk, is  $p_i \propto k_i$ ), and according to Eq. (9) the computational timescale for hubs is much longer than lower-degree nodes. Furthermore, with increasing noise, the error in the estimation of the mean-field is enhanced due to the greater number of neighbors of a hub as compared to nodes in the Poisson graph.

The linear dependence of the viability on the noise, the absence of any plateau, and a constant VpB is in stark contrast with the results seen in the forager model [43]. There, the viability plateau—marked by a peak in the VpB—differentiated the region of semantic and syntactic information. Correlations above the threshold were irrelevant to the forager’s viability. In this setting, however, every bit of syntactic information is semantic. All correlations the agent has with the environment is essential to the viability of the combined agent-environment system.

#### IV. DISCUSSION

The goals of this paper have been twofold. First we propose a general roadmap towards applying semantic information theory (SIT) theory to dynamical systems. Building on [38, 43] we articulate the steps required to cast a system into a form in which one can go beyond syntactic measures of information and consider instead how much of that information contributes to a systems self-maintenance (i.e. viability). Broadly, the procedure involves separating the system into agent-environment sub-systems; defining system dynamics; defining a measure of viability; identifying the state space of correlations between agent and environment such that information theoretic measures may be applied; defining a procedure to *intervene* in the dynamics; computing the semantic content and viability per bit from the ensemble of intervened trajectories. In this way a system and its dynamics can be analyzed as agent-environment correlations directly responsible for an agent’s effectiveness at maintaining itself, the environment, or both, far-from-equilibrium. As we have noted it is the the equilibrium state in question that provides the basis for a semantic interpretation of this information. Thus determination of such equilibria becomes an essential step in the applying SIT to a system. In some cases such equilibria may be obvious, such as the death of an agent [43], however, as we have shown in this paper it is possible that the equilibria of interest, and hence proper viability functions, may require more effort to determine.

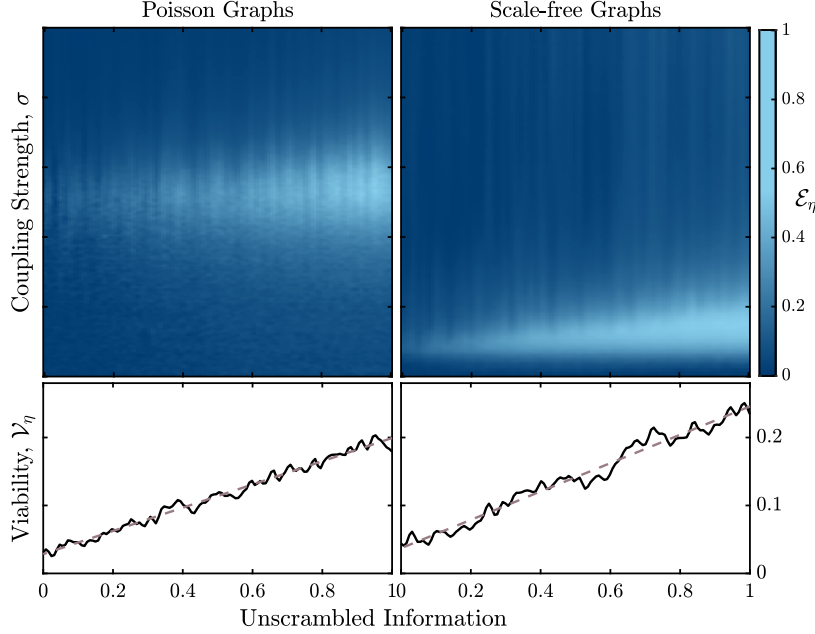


FIG. 4. The noised efficacy Eq. (17) (top panels) as a function of unscrambled information (measured in bits) and coupling  $\sigma$  for Poisson graphs (left), and scale-free graphs (right). The noised viability Eq. (18) is plotted in the bottom panels as a function of unscrambled information. The pink dashed lines in these are the best fit linear models, giving a viability per bit (VpB) of  $0.171 \pm 0.002$ , and  $0.209 \pm 0.003$  for Poisson and scale-free graphs respectively.

Our second goal was to operationalize the road map by exploring a specific model to demonstrate how SIT can bring new insights to previously studied problems. Loosely motivated by biological models such as the neurodynamics of epilepsy and other biologically pathological states, we introduced an agent-based variant of the well-known Kuramoto model. Treating the original model on an arbitrary network as an environment, with an exogenously dependent coupling, an agent is introduced tasked with preventing/delaying the onset of synchronization when the environmental coupling exceeds the critical value. The modified system is a stochastic version of the original model where the effect of the agent is to function as a heat bath that deforms the distribution of frequencies for the oscillators, thus delaying the onset of synchronization. Articulating the resulting correlational structure for agent and environment (the oscillators), allows us to cast the model in a novel computational (information theoretic) perspective, where the agent-environment dynamics can be thought of as analyzing a communication channel. Adding noise to this channel enables the calculation of the system's viability as a function of the level of scrambling of the channel and the viability per bit. Unlike previous explorations of semantic information [43], our results showed no semantic threshold. Instead we find a smooth linear decrease in viability with increased scrambling of the communication

channel. The results indicate that in this case, syntactic and semantic information are indistinguishable; every bit of information in the communication channel between the agent and environment is essential for the system's viability.

In order for an agent to act on information about its environment, it must be able measure this information via some kind of a sensor. The presence or absence of a semantic threshold in a system is then related to the fidelity of the sensor and how it is optimized with respect to the environment. The difference between the forager model and the control-feedback Kuramoto model may well be due to the fact that the sensor in the former case is over-optimized with respect to its environment, whereas in the latter case it senses *only* the information it needs to maintain viability. In biological systems, evolutionary adaptations have led to sensors in organisms with varying amounts of fidelity [68]. For instance, mice, which are nocturnal creatures, cannot see particularly well at night, but have evolved to adopt large ears that give them excellent hearing [69]. Therefore, explorations of SIT on real biological systems may or may not display a semantic threshold depending on the organism, its evolutionary history, and the context in which a viability function is defined. The connection between sensor fidelity and semantic information will be the subject of future explorations.

## Appendix A: Simulation methodology

To acquire the data discussed in this paper we performed simulations written in MATLAB and run on the Bluehive cluster at the University of Rochester. For the environment we constructed 1024 distinct graphs for each of the 256 values of the coupling,  $\sigma \in [0, 1]$ . The environments were initialized with random phases drawn uniformly, and random natural frequencies drawn from a Gaussian distribution with unit standard deviation. Using  $\Delta t = 1/16$ , each environment was run for 1500 timesteps to ensure the decay of any transients; data was then collected for the following 512 timesteps.

With the introduction of the agent,  $\alpha = 0.5$   $\beta = 0.01$ , the number of distinct graphs was reduced to 32, leaving the other numbers mentioned above the same. Furthermore, the experiments were now done for an additional 128 values of the scrambling parameter,  $\eta$ . For simulations with and without agents, the underlying graphs were either Poisson or scale-free. The graphs were constructed via the configuration model [64]. The resulting graphs had  $N = 1000$  nodes and average degrees of  $\langle k \rangle \approx 4$ .

## Appendix B: Derivation of Continuum Dynamics

The agent moves between nodes on a timescale  $\tau$ . During a time interval  $\Delta t$ , the agent makes  $J = \Delta t / \tau = \beta N \Delta t$  jumps between nodes. Due to the topology of the environment the agent visits nodes with higher degree more often than those with lesser degree. The probability of visiting a node  $i$  is proportional to its degree,  $p_i \propto k_i$  (with normalization  $N \langle k \rangle$ ). Each visit results in a perturbation of strength  $\alpha$ , so the expected perturbation to that node is  $\Delta \theta_i = \alpha p_i J = \alpha \kappa_i \beta k_i \Delta t / \langle k \rangle$ . Since visits are rare, the perturbations are a Poisson arrival process. On timescales much larger than a single jump, the expected number of visits is high enough to model the Poisson process as a fixed rate with Gaussian fluctuations. Taken together, this means that we can think of the agent's actions on each oscillator as approximated by a continuous perturbation of strength

$$\left. \frac{d\theta_i}{dt} \right|_{\text{cont.}} = \alpha \beta \kappa_i \frac{k_i}{\langle k \rangle} \quad (\text{B1})$$

modulated by, heuristically, a stochastic fluctuation of size

$$\left. \frac{d\theta_i}{dt} \right|_{\text{stoch.}} = \sqrt{\alpha \beta \frac{k_i}{\langle k \rangle}} \frac{1}{\sqrt{\Delta t}} \quad (\text{B2})$$

Note the presence of the  $\sqrt{\Delta t}$  above, which motivates our quantification of this heuristic by the replacement of this term with a Wiener process.

## Appendix C: Review of Fully Connected Model

In this appendix we review the calculation of the critical coupling in the original fully connected model. There we have that  $\sigma = K/N$ ; the coupling needs to scale inversely with the number of nodes because in a fully-connected graph the number of connections, by definitions, scales with  $N$ . Our starting point is therefore Eq. (4), the mean field equation of motion. We work under the simplifying assumption of the long-time, thermodynamic limit,  $t \rightarrow \infty, N \rightarrow \infty$ , so that fluctuations in the synchronization order parameter,  $r$ , vanish, allowing us to treat it as constant. In what follows we will derive a self-consistency constraint on the synchronization, from which everything else will follow.

Consider an oscillator with natural frequency  $\omega$ . If  $|\omega| > Kr$ , then  $\theta$  never vanishes, and the oscillator is unsynchronized. On the other hand if  $|\omega| \leq Kr$ , the oscillator synchronizes, approaching a phase of  $\theta \rightarrow \phi + \sin^{-1} \omega / Kr$ . We use these facts to break apart the sum in the definition of the synchronization into two sums, one over the synchronized, and the other over the unsynchronized, oscillators

$$\begin{aligned} r e^{i\phi} &= \frac{1}{N} \sum_i e^{i\theta_i} \\ &= \frac{1}{N} \sum_{i|\omega_i > Kr} e^{i\theta_i} + \frac{1}{N} \sum_{i|\omega_i \leq Kr} e^{i\theta_i} \end{aligned}$$

The thermodynamic limit assumption allows us to disregard the first term - the unsynchronized oscillators will be distributed uniformly across phases, cancelling. For the second term, we use the long-time assumption to set the phases to their synchronized values noted above, resulting in

$$r = \frac{1}{N} \sum_{i|\omega_i \leq Kr} e^{i \sin^{-1} \frac{\omega_i}{Kr}}$$

The thermodynamic limit assumption here allows us to replace the sum with an appropriate integral over the frequency distribution, which when combined with some elementary trigonometric identities, results in

$$r = \int_{-Kr}^{Kr} d\omega g(\omega) \left( \sqrt{1 - \frac{\omega^2}{K^2 r^2}} + i \frac{\omega}{Kr} \right)$$

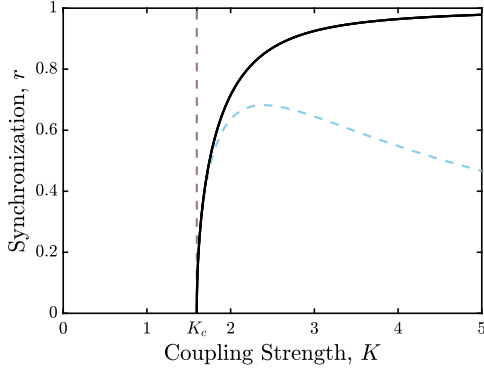


FIG. 5. Synchronization in the fully connected Kuramoto model with a Gaussian distribution of natural frequencies. The vertical line is at the critical coupling,  $K_c = 2\sqrt{2/\pi}$ . The dashed curve is the second order approximation.

Since we work with symmetric frequency distributions, the imaginary piece of the above vanishes. In what remains, we perform the substitution  $\omega = Krx$ , resulting in the self-consistency integral constraint

$$\frac{1}{K} = 2 \int_0^1 dx \sqrt{1-x^2} g(Krx) \quad (C1)$$

In the case of a standardized Gaussian, the integral can be performed leading to an algebraic self-consistency constraint,

$$\frac{1}{K} = \sqrt{\frac{\pi}{8}} e^{-\frac{K^2 r^2}{4}} \left( I_0\left(\frac{K^2 r^2}{4}\right) + I_1\left(\frac{K^2 r^2}{4}\right) \right), \quad (C2)$$

where the  $I_\nu$  are modified Bessel functions. This transcendental equation is plotted on the  $(K, r)$  plane, showing the well-known synchronization phase transition in figure 5.

For more general symmetric distributions, proximity to the critical point is still amenable to analysis. When  $K > K_c$ ,  $r > 0$ , and as  $K \rightarrow K_c$  from above,  $r \rightarrow 0$ . This observation motivates an expansion in  $Kr$  for the frequency distribution

$$g(Krx) = \sum_{n=0}^{\infty} \frac{1}{2n!} g^{(2n)}(0) (Kr)^{2n} x^{2n}, \quad (C3)$$

where we have used the symmetry of  $g$  as an even function. Plugging into the self-consistency constraint results in integrals easily recognizable as Euler beta functions, which massaged with several Euler gamma function identities result in

$$\frac{1}{K} = \frac{\pi}{2} \sum_{n=0}^{\infty} \frac{g^{(2n)}(0) K^{2n} r^{2n}}{4^n n! (n+1)!}. \quad (C4)$$

Setting  $K = K_c$  so that  $r = 0$  gives the critical coupling in terms of the center of the frequency distribution,

$$\frac{1}{K_c} = \frac{\pi}{2} g(0). \quad (C5)$$

The next order of the calculation,

$$\begin{aligned} \frac{1}{K} &= \frac{1}{K_c} + \frac{\pi}{16} g''(0) K^2 r^2 \\ &\Downarrow \\ r^2 &= 8 \frac{g(0)}{g''(0)} \frac{K - K_c}{K^3} \end{aligned} \quad (C6)$$

gives a critical exponent of  $1/2$ .

- 
- [1] E. Schrodinger, *What is life* (Cambridge: Cambridge University Press, 1944).
  - [2] J. D. Watson and F. H. Crick, *Nature* **171**, 737 (1953).
  - [3] P. Godfrey-Smith, “Information in biology,” in *The Cambridge Companion to the Philosophy of Biology*, Cambridge Companions to Philosophy, edited by D. L. Hull and M. Ruse (Cambridge University Press, Cambridge, 2007) pp. 103–119.
  - [4] H. Mattingly, K. Kamino, B. Machta, and T. Emonet, *Nature physics* **17**, 1426 (2021).
  - [5] B.-O. Küppers, *Information and the Origin of Life* (Mit Press, 1990).
  - [6] C. Adami, *Physics of Life Reviews* **1**, 3 (2004).
  - [7] S. Uda, *Biophysical reviews* **12**, 377 (2020).
  - [8] A. Gohari, M. Mirmohseni, and M. Nasiri-Kenari, *IEEE Transactions on Molecular, Biological and Multi-Scale Communications* **2**, 120 (2016).
  - [9] A. Rhee, R. Cheong, and A. Levchenko, *Physical biology* **9**, 045011 (2012).
  - [10] G. Tkačik and W. Bialek, *Annual Review of Condensed Matter Physics* **7**, 89 (2016).
  - [11] M. C. Donaldson-Matasci, C. T. Bergstrom, and M. Lachmann, *Oikos* **119**, 219 (2010).
  - [12] O. Rivoire and S. Leibler, *Journal of Statistical Physics* **142**, 1124 (2011).
  - [13] R. M. Hazen, P. L. Griffin, J. M. Carothers, and J. W. Szostak, *Proceedings of the National Academy of Sciences* **104**, 8574 (2007).
  - [14] D. R. Sowinski, J. Carroll-Nellenback, J. DeSilva, A. Frank, G. Ghoshal, and M. Gleiser, *Entropy* **24**, 1378 (2022).



- [15] S. Oh, E. F. Bowen, A. Rodriguez, D. Sowinski, E. Childers, A. Brown, L. Ray, and R. Granger, arXiv preprint arXiv:2011.00088 (2020).
- [16] E. F. Bowen, A. M. Rodriguez, D. R. Sowinski, and R. Granger, *Journal of Vision* **22**, 4 (2022).
- [17] C. E. Shannon, *The Bell system technical journal* **27**, 379 (1948).
- [18] G. Schlosser, *Synthese* **116**, 303 (1998).
- [19] M. Mossio, C. Saborido, and A. Moreno, *The British Journal for the Philosophy of Science* **60**, 813 (2009).
- [20] X. E. Barandiaran and M. D. Egbert, *Artificial Life* **20**, 5 (2014).
- [21] M. Egbert, M. M. Hanczyc, I. Harvey, N. Virgo, E. C. Parke, T. Froese, H. Sayama, A. S. Penn, and S. Bartlett, *Origins of Life and Evolution of Biospheres*, 1 (2023).
- [22] J. K. D. Polani, T. Martinez, *An information-theoretic approach for the quantification of relevance* (Springer, Berlin, Germany, 2001).
- [23] E. Thompson and M. Stapleton, *Topoi* **28**, 23 (2009).
- [24] C. L. Nehaniv, D. Polani, K. Dautenhahn, R. te Beekhorst, and L. Cañamero, in *Proceedings of the Eighth International Conference on Artificial Life*, ICAL 2003 (MIT Press, Cambridge, MA, USA, 2002) pp. 345–349.
- [25] J. Barham, *Biosystems* **38**, 235 (1996).
- [26] T. W. Deacon, *Cognitive Semiotics* **1**, 123 (2007).
- [27] P. A. Corning, *Systems Research and Behavioral Science: The Official Journal of the International Federation for Systems Research* **24**, 297 (2007).
- [28] M. Gleiser and D. Sowinski, *The Map and the Territory: Exploring the Foundations of Science, Thought and Reality*, 141 (2018).
- [29] J. A. Acebrón, L. L. Bonilla, C. J. Pérez Vicente, F. Ritort, and R. Spigler, *Reviews of Modern Physics* **77**, 137 (2005).
- [30] D. García-Selfa, G. Ghoshal, C. Bick, J. Pérez-Mercader, and A. P. Muñuzuri, *Chaos, Solitons & Fractals* **145**, 110809 (2021).
- [31] F. Cooper, G. Ghoshal, A. Pawling, and J. Pérez-Mercader, *Physical Review Letters* **111**, 044101 (2013).
- [32] S. Mimar, M. M. Juane, J. Park, A. P. Muñuzuri, and G. Ghoshal, *Physical Review E* **99**, 062303 (2019).
- [33] J. E. COHEN, *Nature* **270**, 165 (1977).
- [34] N. Rooney, K. McCann, G. Gellner, and J. C. Moore, *Nature* **442**, 265 (2006).
- [35] J. C. Xavier, W. Hordijk, S. Kauffman, M. Steel, and W. F. Martin, *Proceedings of the Royal Society B: Biological Sciences* **287**, 20192377 (2020).
- [36] J. C. Blain and J. W. Szostak, *Annual Review of Biochemistry* **83**, 615 (2014), PMID: 24606140, <https://doi.org/10.1146/annurev-biochem-080411-124036>.
- [37] S. Mimar, M. M. Juane, J. Mira, J. Park, A. P. Muñuzuri, and G. Ghoshal, *Physical Review Research* **3**, 023241 (2021).
- [38] A. Kolchinsky and D. H. Wolpert, *Interface focus* **8**, 20180041 (2018).
- [39] C. Rovelli, in *Wandering Towards a Goal*, The Frontiers Collection (Springer, Cham, 2018) pp. 17–27.
- [40] D. R. Sowinski, M. D. McGarry, E. E. Van Houten, S. Gordon-Wylie, J. B. Weaver, and K. D. Paulsen, *Frontiers in physics* **8**, 617582 (2021).
- [41] R. L. Stratonovich, *Theory of Information and its Value*, edited by R. V. Belavkin, P. M. Pardalos, and J. C. Principe (Springer International Publishing, Cham, 2020).
- [42] C. E. Shannon *et al.*, *IRE Nat. Conv. Rec* **4**, 1 (1959).
- [43] D. R. Sowinski, J. Carroll-Nellenback, R. N. Markwick, J. Piñero, M. Gleiser, A. Kolchinsky, G. Ghoshal, and A. Frank, *PRX Life* **1**, 023003 (2023).
- [44] O. Bénichou and S. Redner, *Physical review letters* **113**, 238101 (2014).
- [45] U. Bhat, S. Redner, and O. Bénichou, *Physical Review E* **95**, 062119 (2017).
- [46] O. Bénichou, M. Chupeau, and S. Redner, *Journal of Physics A: Mathematical and Theoretical* **49**, 394003 (2016).
- [47] U. Bhat and S. Redner, *Journal of Statistical Mechanics: Theory and Experiment* **2022**, 033402 (2022).
- [48] Y. Kuramoto, in *International Symposium on Mathematical Problems in Theoretical Physics: January 23–29, 1975, Kyoto University, Kyoto/Japan* (Springer, 1975) pp. 420–422.
- [49] Y. Zheng, G. Wang, K. Li, G. Bao, and J. Wang, *Clinical Neurophysiology* **125**, 1104 (2014).
- [50] P. Uhlhaas and W. Singer, *Neuron* **52**, 155 (2006).
- [51] M. Siegel, T. H. Donner, and A. K. Engel, *Nature Reviews Neuroscience* **13**, 121 (2012).
- [52] G. Ghoshal, A. P. Muñuzuri, and J. Pérez-Mercader, *Scientific Reports* **6**, 19186 (2016).
- [53] W. Penfield and H. Jasper, *Epilepsy and the Functional Anatomy of the Human Brain* (Little, Brown and co., Boston, U.S.A, 1954).
- [54] D. M. Abrams and S. H. Strogatz, *Physical Review Letters* **93**, 174102 (2004).
- [55] Y. Zhang and A. E. Motter, *Physical Review Letters* **126**, 094101 (2021).
- [56] O. E. Omel'chenko, *Nonlinearity* **31**, R121 (2018).
- [57] T. M. Cover and J. A. Thomas, *Elements of Information Theory (Wiley Series in Telecommunications and Signal Processing)* (Wiley-Interscience, USA, 2006).
- [58] Z. Chen, S. Kelty, A. G. Evsukoff, B. F. Welles, J. Bagrow, R. Menezes, and G. Ghoshal, *Nature Communications* **13**, 1922 (2022).
- [59] T. Schreiber, *Phys. Rev. Lett.* **85**, 461 (2000).
- [60] R. E. Mirollo and S. H. Strogatz, *SIAM Journal on Applied Mathematics* **50**, 1645 (1990).
- [61] S. H. Strogatz, D. M. Abrams, A. McRobie, B. Eckhardt, and E. Ott, *Nature* **438**, 43 (2005).
- [62] A. Moiseff and J. Copeland, *Science* **329**, 181 (2010).
- [63] B. Li and K. M. Wong, *Physical Review E* **95**, 012207 (2017).
- [64] M. Newman, *Networks* (Oxford University Press, Oxford, United Kingdom, 2018).
- [65] F. A. Rodrigues, T. K. D. Peron, P. Ji, and J. Kurths, *Physics Reports* **610**, 1 (2016).
- [66] B. Sonnenschein, M. A. Zaks, A. B. Neiman, and

- L. Schimansky-Geier, *The European Physical Journal Special Topics* **222**, 2517 (2013).
- [67] B. Sonnenschein and L. Schimansky-Geier, *Physical Review E* **88**, 052111 (2013).
- [68] H. A. Orr, *Nature Reviews Genetics* **6**, 119 (2005).
- [69] H. Morsli, D. Choo, A. Ryan, R. Johnson, and D. K. Wu, *The Journal of Neuroscience* **18**, 3327 (1998).